Journal of Materials Chemistry C

Accepted Manuscript

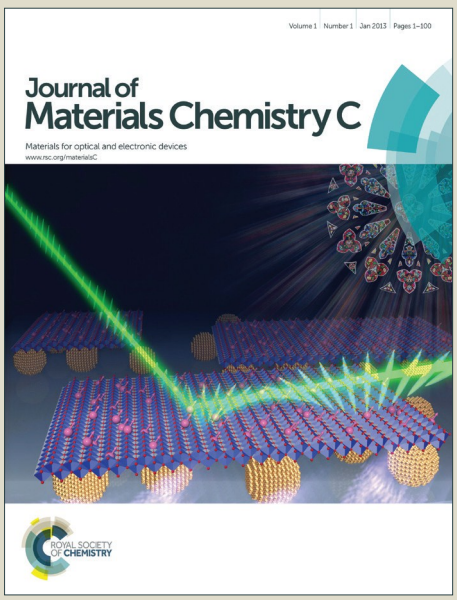

ROYAL SOCIETY OF CHEMISTRY

www.rsc.org/materialsC

Light-controlled C_2H_2 gas sensing based on Au-ZnO nanowires with plasmon-enhanced sensitivity at room-temperature

Z. Q. Zheng [a], B. Wang [b*], J. D. Yao [a] and G. W. Yang [a*]

[a] *State Key Laboratory of Optoelectronic Materials andTechnologies,Nanotechnology Research Center, School of Physics & Engineering, Sun Yat-sen University, Guangzhou510275, Guangdong, P. R. China.*

[b] *Institute of Micro-nano Optoelectronic Technology，Shenzhen Key Lab of Micro-nano Photonic Information Technology，College of Electronic Science and Technology, Shenzhen University, Shenzhen, 518060, Guangdong, P. R. China.*

*Corresponding authors: stsygw@mail.sysu.edu.cn and wangbing@szu.edu.cn

Abstract

We have experimentally demonstrated a visible light-controlled sensing response of the Au-ZnO nanowires for C_2H_2 gas at room temperature by the plasmon-enhanced sensitivity, in which Au nanoparticles were coated on the surface of ZnO nanowires. The ZnO nanowires without Au nanoparticles showed a normal n-type response, whereas the Au coated ZnO nanowires exhibited a concentration-dependent and time-dependent p–n transition response for the sensing response to C_2H_2 gas at room temperature. This unconventional sensing behavior can be explained by the formation of a surface inversion layer. Meanwhile, this sensing can be modulated and the response was significantly enhanced at room temperature under visible light illumination. This light-controlled sensing response from the Au-ZnO nanowires was attributed to that the visible light excites the surface plasmon resonance of Au nanoparticles on the surface of ZnO nanowires, and it can inject hot electrons into the conduction band of ZnO. These results hinted the potential application of the as-fabricated sensor in monitoring C_2H_2 gas at room temperature, and opened up new approaches for developing new generation of visible light modulated gas sensor.

Keywords: light-controlled gas sensing, ZnO nanowires, Au nanoparticles, plasmon.

Introduction

In recent years, with the increasing concerns on the effects of pollution on health and safety, gas sensors based on semiconducting metal oxide nanostructures, especially ZnO nanostructures, have received tremendous attention because of their high sensitivity, excellent chemical stability and fabrication flexibility[1-6]. However, most of the sensors have to operate at a high temperature to achieve excellent sensing performance[7-9]. In addition to increase energy consumption, the high operation temperature can limit its practical applications in some situations, such as, flammable and explosive environments. What is more, high operations temperature can lead to long-term reliability problems due to the growth of oxide grains[10]. Therefore, developing a new generation of gas sensors with low power consuming, especially working in a continuous mode at room temperature is a quite attractive and challenge task.

For operating at room temperature, a range of techniques have been used, such as, noble metal doping the sensing materials[11, 12], applying an electrostatic field on the sensor[13], and illuminating the sensors with UV light radiation[14]. Among these techniques, UV light irradiation has attracted increasing attention as a promising strategy to achieve room temperature response[15-17]. However, UV light source is expensive and UV ray is harmful on human health, resulting in increasing cost and restricting its practical applications in gas-sensing region. Compared with UV light sources, the use of solar energy as the operating source is the optimal choice to reduce

its cost as well as avoiding UV exposureof the human body[18].

Very recently, the visible light excitation of the surface plasmon resonance (SPR) of Au nanoparticles (NPs) loaded on ZnO nanostructures has been found to cause the electron injection from Auto ZnO by so-called "hot electron"[19, 20]. And this effect has been reported to apply to the solar water splitting[21-23] and dye-sensitized solar cells[24-26]. Nevertheless, up to now, there are much few reports on applying this effect to enhance the gas sensing performance while ZnO is the most commonly used material for gas sensors. For these issues, in this contribution, we report the sensing response of the ZnO nanowires (NWs) coated by Au NPs under visible light radiation for acetylene (C_2H_2) gas at room temperature, and we demonstrate avisible light-controlled sensing response of the Au-ZnO NWs for C_2H_2 gas at room temperature by the plasmon-enhanced sensitivity. Additionally, a type of concentration-dependent and time-dependent p–n transition for this sensing response to C_2H_2 gas is observed in the Au-ZnO NWs gas sensors, and the relevant physical understandings are proposed.In this way, we develop a novel visible light modulated C_2H_2 gas sensor.

Experimental

Preparation and characterization of the sensing materials. ZnO NWs is prepared using the chemical vapor deposition reported in our previous work[27, 28]. In detail, commercial ZnO and active carbon powders are mixed in a 1:1 weight ratio as

the reaction source and loaded on one end of a small quartz tube, silicon substrates covered with anAu layer are placed on the other end of the small quartz tube. Then, they are pushed into a larger quartz tube in a horizontal tube electric furnace. After the whole system is evacuated for 20 minutes; the nitrogen gas is introduced into the system as the carrier gas at the rate of 25 sccm and the pressure is kept at 90 Torr. Then, the system is rapidly heated to 950 ℃ and maintain for 1 hour. Finally, the system is cooled down to room temperature in several hours. A white film is observed on silicon substrates when they are moved out, and they are ZnO NWs. Then, we coat various amounts of Au NPs on the surface of the as-prepared ZnO NWs by sputtering. The sputter current is 40 mA, and the deposition time is 60 s. Sequentially, the Au-ZnO NWs are annealed at 500 °C for 1 hour in air, which are the Au-ZnO NWs in our case.

Field-emission scanning electron microscopy (FESEM, ZEISS AURIGA-4523) is used to characterize the morphology of the ZnO NWs and Au-ZnO NWs samples, and their phase purity and structure are characterized by X-ray diffraction (XRD, Rigaku D-MAX 2200 VPC) with Cu Kα radiation scanning from 20-80^{o} at room temperature. The UV-vis diffuse reflectance spectrum of the samples are measured by using an ultraviolet–visible–near infrared (UV-Vis-NIR) spectrophotometer (Perkin Elmer, Lambda 950), while $BaSO_4$ is used as the reference.

Gas sensing measurement. Visible light modulated gas sensing response is measured by the JF02E gas sensing characterization system (Gyjf Technology Co.

Ltd., P. R. China) as reported in our previous work[27]. Certain concentration of C_2H_2 gas or clean air is periodical passed into the test chamber based on computer-controlled mass flow controllers (MFCs), and the total flow rate is maintained at 500 sccm. During the measurements, 532 nm monochromatic light as the excitation light source is irradiated on the sensor through the quartz window of the test chamber, and all the measurements above are carried out at room temperature.

Results and Discussion

Morphology characterization of the sensing materials. Morphology and structure of the as-prepared samples are shown in Fig. 1. Clearly, the nanowires cover the whole area of the Si substrate and their length can reach up to several tens of micrometers as shown in Fig. 1a. High magnified FESEM image in Fig. 1b shows the diameter of the nanowires is about 100 nm, and they are very uniform in size and shape. Fig. 1c shows the high magnified FESEM image of the Au-ZnO NWs. We can see that Au NPs with the size approximately 80 nm are uniformly deposited on the surface of nanowires.

Phase purity and structure of the as-prepared samples are investigated by XRD. As shown in Fig.1d, all the diffraction peaks can be indexed as the typical hexagonal wurtzite ZnO (JCPDS NO. 36-1451)[29, 30], and the sharp diffraction peaks indicate its high purity. In addition to the peaks of ZnO, the diffraction peak of the Si (211) plane is from the substrate. And the two weak diffraction peaks attributed to the Au (111)

and Au (200) planes (JCPDS NO. 04-0784) are also observed in the spectrum of the Au-ZnO NWs, which further confirm the present of Au NPs on the surface of ZnO NWs. Furthermore, no shifts in the position of diffraction peaks are observed, indicating that Au is deposited on the surface of ZnO NWs through the formation of Au-ZnO nanocomposites rather than Au atom substitutes for Zn^{2+} or as an interstitial atom[3].

The optical properties of the ZnO NWs without Au NPs and Au-ZnO NWs are investigated by measuring their UV–vis absorption spectra. As shown in Fig. 1e and f, both the two curves show an absorption band at 370 nm which is corresponding to the band edge absorption of ZnO. In addition, the Au-ZnO NWs shows another strong broad absorption peakat approximately 530 nm, which is due to the surface plasmon resonance of Au NPs[31], while the ZnO NWs also shows a weak absorption peak in this area (as the blue-color circle), which should be ascribed to Au used for catalysis synthesis ZnO NWs. It is worth noticing that in Fig. 1f, there exists a distinct spectral splitting around 510 nm that can be identified as arising from Rabi oscillations[32].

Senor fabrication. The fabrication of the C_2H_2 sensor is as follows. Two gold electrodes are deposited on one sides of the alumina ceramic substrate, the distance between them is 1 mm, and a Pt heater is placed on the other side of the substrate, so asto provide appropriate working temperature for the sensor. Afterwards, the ZnO NWs and Au-ZnO NWs are dropped coating on the substrate. After taking the substrate into a horizontal tube electric furnace and annealing at 300 °C for 3 hours,

and packaging on a metal stent, the C_2H_2 sensor is fabricated. The schematic diagrams and photographs of the C_2H_2 sensor are shown in Fig. 2.

Visible light modulated gas sensing performance. We fabricated the gas sensors with the as-prepared ZnO nanostructures. As the ZnO NWs sensor exhibits no gas sensing activity to C_2H_2 gas at room temperature, we investigate the dynamics response of the ZnO NWs sensor towards various concentrations of C_2H_2 diluted by air at the working temperature of 130 ^oC in dark. Note that the temperature of the sensor is measured by contacting a thermocouple to the upper side of the sensor element. As shown in Fig. 3a, a decrease of the resistance is registered when the sensor is exposed to the gas for all the tested concentrations. This is the typical behavior of an n-type semiconductor-based gas sensor response to reducing gases, and it is generally in the case of ZnO nanostructures[33-35]. The effect of the working temperature on the sensing response is also studied later.

An unusual but reversible behavior is instead observed when exposing the Au-ZnO NWs sensor to C_2H_2 gas at room temperature in dark. In Fig. 3b, we can find that the type of sensing response depends on the concentration of C_2H_2 gas. This Au-ZnO NWs sensor shows a reverse p-type sensing response to 25 ppm C_2H_2 gas, and a borderline response to 50 ppm C_2H_2 gas. Within creasing C_2H_2 concentration from 50 to 500 ppm, the sensor switches to the n-type response and the response magnitude improves dramatically. More precisely, a time-dependent p–n transition response can also be observed if we watch the curve of response to 50-500 ppm C_2H_2

gas more in detail. As shown in the red-color circle in Fig. 3b, upon exposed to C_2H_2 gas, the resistance of the sensor is subjected to a sharply increase (p-type response), which is then compensated by decreasing to a relatively constant value below the baseline (n-type response). After C_2H_2 gas is shut off, the resistance of the sensor drops rapidly (p-type response), and then recovers to the baseline resistance (n-type response). This time-dependent p-n transition response can be investigated more by taking a closer look at the individual sensing response to 200 ppm C_2H_2 gas as shown in Fig. 3c. Specifically, when 200 ppm C_2H_2 gas diluted by air is passed into the test chamber, the sensor shows a p-type response in the first 31 seconds, and then switches to an n-type response after 155 seconds because of the inversion of carriersfrom p to n-type.

We also study the sensing performance of the sensor to C_2H_2 gas under 532 nm light. There is nearly no change in the response of the ZnO NWs sensor to C_2H_2 gas under 532 nm light. Fig. 3d depicts the dynamics response of the Au-ZnO NWs sensor towards various concentrations of C_2H_2 gas at room temperature under 532 nm light illumination. We can observe that it always shows an n-type sensing response to C_2H_2 gas for concentrations from 25 to 500 ppm, and the concentration-dependent p-n transition is disappeared. On the other hand, the time-dependent p-n transition responseis still remains, while it is not as obvious as that in dark. Details is shown in Fig. 3e, at the initial 200 ppm C_2H_2 gas is pulled in the chamber, in the first 20 seconds, there also have a sharply increase in the resistanceup the baseline (p-type response). Subsequently, the resistance drops rapidly, just after 51 seconds because of

the inversion of carriers, and the response switches to n-type. Moreover, the magnitude of resistance decrease under 532 nm light irradiation is much larger than that in dark. If we increase the light intensity, the time-dependent p-n transition response will also disappear as shown in Fig. 3f. At this time, the resistance decreases directly upon exposure to C_2H_2 gas and recovers completely to the initial value upon the removal of C_2H_2 gas, and then the Au-ZnO NWs sensor becomes a normal n-type gas sensor (Fig. 3g).

To observe clearly the results above, the gas-sensing response of the Au-ZnO NWs sensor is calculated and shown in Fig. 3h. We define the response of the sensorusing the expression of Response% = $(R_a- R_g)/R_a*100\%$[36], where R_a and R_g are the resistance of the sensor before and in exposing to the tested gas, respectively. Clearly, our sensor shows the responses ranging from -1.84% to 19.4% in dark. In contrast, under a 532 nm light irradiation and a stronger light irradiation, respectively, it shows responses ranging from 8.15% to 46.9% and from 7.64% to 35.64%, respectively, at C_2H_2 gas concentrations of 25-500 ppm at room temperature. Therefore, we can clearly observe that visible light illumination not onlygreatly enhances the gas sensing performance, but also transforms the response type at room temperature.

Gas sensing mechanism of light-controlled sensor. Different kinds of response inversion phenomena in gassensors have been reported so far[37-39], while the explanation for that is still debatable. In order to clarify the detail mechanism of the

transition behavior between p-type and n-type in our case, the conductivity-type diagrams are schematically shown as Fig. 4. As indicated before, ZnO NWs is generally an n-type semiconductor ($n > n_i > p$) and its corresponding band diagram is shown in the left of Fig. 4a, where the Fermi level (E_f) is above the intrinsic level (E_i). When ZnO NWs are exposed to air in dark at room temperature, oxygen molecules will adsorb on the surface and capture electrons from the conduction band of ZnO to form chemisorbed oxygen anions O_2^- as Eq. (1)[40], resulting inthe upward of the intrinsic level and the formation of a low-conductivity depletion region near the surface and narrow the conduction channels in ZnO NWs. By heating the sensor to 130 ^oC, such a behavior above is more notabledue to that the adsorbed oxygen molecules will capture more electrons from the conduction band at moderate temperature as show in the middle of Fig. 4a. When C_2H_2 gas is injected into the test chamber, oxygen anions O_2^- would react with the reducing gas and release electrons back to the conduction band of ZnO NWs. The reaction can be depicted as Eq. (2), and the surface depletion layer width is reduced, the position of the intrinsic level is brought downward as shown in the right of Fig. 4a.

$$O_2 + 2e^- \longrightarrow O_{2\,(ads)}^- \quad (1)$$

$$2C_2H_2 + 5O_{2\,(ads)}^- \xrightarrow{heat} 4CO_2 + 2H_2O + 5e^- \quad (2)$$

After depositing Au NPs catalyst on the surface, Au NPs could increase the adsorption of oxygen molecules due to its spillover effect. This chemical mechanism of Au NPs will make more electrons be trapped, and then the depletion layer will be

thicker[41]. The strong absorption of oxygen molecules results in the formation of aninversion layer near the surface, where the Fermilevel is below the intrinsic level (n $<n_i<$ p) as shown in the left of Fig. 4b. In this inversion layer, hole is the majority carriers, which result in a p-type conductivity layer. Moreover, Au NPs could catalytically activate the dissociation of oxygen molecular[30], and this progress would greatly decrease the working temperature.

Upon low concentration of C_2H_2 gas is pushed in, it will be oxidized to CO_2 and H_2O by the chemisorbed O_2^-as Eq. (3) and transfer some electrons back to the semiconductor, leading to reduce the width of the inversion layer and increase the resistance, but the Fermi levelis still below the intrinsic level (n $<n_i<$ p) as shown in the middle of Fig. 4b. With the introduction of higher concentration of gas, C_2H_2 gas would further react with the chemisorbed O_2^- and transfer more electrons back to the semiconductor, resulting in the electron concentration (n) increasing. Then n would reach the intrinsic level (n $=n_i=$p), and subsequently become larger than the hole concentration (n$>n_i>$p) with increasing exposures to C_2H_2 gas, which cause a depletion layer instead of the inversion layer as shown in the right of Fig. 4b. Then, the concentration-dependent p-n transition response is observed. As the inversion of carriers should take time, the time-dependentp-n transition response is also observed. Therefore, the results are in agreement with the experimental results in Fig. 3b. The chemisorbed oxygen ion ($O_{2\,(ads)}^-$), including the oxygen ion captured by Au NPs catalytic, have the large adsorption energy so as to be stable and difficult to be

removed from the ZnO surface, and then, scarcely react with acetylene molecules at room temperature[42]. Therefore, the gas sensing response in dark is unobvious.

$$2C_2H_2 + 5O_2^-{}_{(ads)} \xrightarrow{Au} 4CO_2 + 2H_2O + 5e^- \quad (3)$$

When the Au-ZnO NWs sensor captures weak visible light illumination, Au NPs would absorb the plasmon-induced irradiation (around 532 nm light) to generate hot electrons and an electromagnetic field. The plasmon-induced hot electrons will inject into the conduction band of ZnO over the Schottky barrier[20], resulting in reducing the width of the inversion layerand leading to downwardthe position of the intrinsic level, but it is remain above the Fermi level ($n < n_i < p$) as shown in the left of Fig. 4c. Meanwhile, the ambient oxygen molecules will react with "hot electrons"as Eq. (4) and result in creating additional visible light-induced oxygen ions.

$$O_2 + e^-{}_{(hv)} \longrightarrow O_2^-{}_{(hv)} \quad (4)$$

Unlike the chemisorbed oxygen ions ($O_2^-{}_{(ads)}$), which are strongly attached to the ZnO NWs surface, the visible light-induced oxygen ions ($O_2^-{}_{(hv)}$) generated by SPR of Au NPs are weakly bound to ZnO NWs, and they are highly reactive and responsible for the room-temperature gas sensitivity[42]. Therefore, upon exposure to C_2H_2 gas, these photo-induced oxygen ions ($O_2^-{}_{(hv)}$) play a major role in the redox reaction at room temperature as Eq. (5), which leading to enhance the gas sensing performance greatly. Moreover, this process brings about large amounts of electrons repopulating the semiconductor, and the rate is much more rapidly than that in dark, resulting in fast brought down ward the position of intrinsic level below the Fermi level ($n > n_i > p$)

as shown in the middle of Fig. 4c. Then, the concentration-dependent p-n transition response is disappeared, while the time-dependent p-n transition responseis not as obvious as that in dark, which are in agreement with the experimental results in Fig. 3d.

$$2C_2H_2 + 5O_2^-{}_{(h\nu)} \xrightarrow{Au} 4CO_2 + 2H_2O + 5e^- \quad (5)$$

With the introduction of stronger visible light illumination, large amounts of the plasmon-induced “hot electrons” will generate and inject into the conduction band of ZnO NWs, which resulting in brought down ward the position of the intrinsic level below the Fermi level ($n > n_i > p$) as shown in the right of Fig. 4c. At this time, the electron concentration is large enough to be the majority carriers, and this sensor becomes a normal n-type gas sensor, which are in agreement with the experimental results in Fig. 3f. As mentioned above, the visible light not only significantly enhances the gas sensing response in comparison with the results in dark, but also effectively modulates the gas sensing type. Therefore, a light-controlling gas sensor is realized by us.

Conclusions

In summary, we have demonstrated the visible light modulated sensing response of the Au-ZnO NWs for C_2H_2 gas at room temperature by in dark and under visible light irradiation. In dark, the ZnO NWs sensor exhibited a normal n-type response to C_2H_2 gas, while the Au-ZnO NWs sensor showed a type of concentration-dependent and time-dependent p–n transition response. This abnormal p-n transition was

ascribed to the strongsurface absorption, resulting in the formationof a surface inversion layer. Compared to those in dark, the responses were significantly enhanced and even transformed the response type at room temperature under visible light irradiation. The reason was that, by absorbing the plasmon-induced irradiation, Au NPs generate hot electrons and then inject them into the conduction band of ZnO over the Schottky barrier, leading to adjusting the position of the intrinsic level. Thus, these studies actually open up new approaches for developing new generation of gas sensor.

Acknowledgements. The National Basic Research Program of China (2014CB931700), Project of Department of Education of Guangdong Province (2013KJCX0165), Outstanding young teacher training project in the institutions of higher learning of Guangdong Province (Yq2013145), Basic Research Project of Shenzhen (JCYJ20140418193546110) and Open Project of Shenzhen Key Laboratory of Micro-nano Photonic Information Technology (MN201405) supported this work.

References

1. R. Ab Kadir, Z. Li, A. Z. Sadek, R. Abdul Rani, A. S. Zoolfakar, M. R. Field, J. Z. Ou, A. F. Chrimes and K. Kalantar-zadeh, *The Journal of Physical Chemistry C*, 2014, **118**, 3129-3139.

2. X. Pan, X. Liu, A. Bermak and Z. Fan, *ACS nano*, 2013, **7**, 9318-9324.

3. J. Cui, D. Wang, T. Xie and Y. Lin, *Sensors and Actuators B: Chemical*, 2013, **186**, 165-171.

4. M. R. Alenezi, S. J. Henley, N. G. Emerson and S. R. Silva, *Nanoscale*, 2014, **6**, 235-247.

5. A. Katoch, J. H. Kim and S. S. Kim, *ACS applied materials & interfaces*, 2014, **6**, 21494-21499.

6. C. M. Chang, M. H. Hon and I. C. Leu, *ACS applied materials & interfaces*, 2013, **5**, 135-143.

7. Q. Zhou, W. Chen, L. Xu and S. Peng, *Sensors*, 2013, **13**, 6171-6182.

8. L. Zhang, J. Zhao, J. Zheng, L. Li and Z. Zhu, *Sensors and Actuators B: Chemical*, 2011, **158**, 144-150.

9. H. Zhang, C. Xu, P. Sheng, Y. Chen, L. Yu and Q. Li, *Sensors and Actuators B: Chemical*, 2013, **181**, 99-103.

10. S. Park, S. An, Y. Mun and C. Lee, *ACS applied materials & interfaces*, 2013, **5**, 4285-4292.

11. S. Park, S. An, H. Ko, S. Lee and C. Lee, *Sensors and Actuators B: Chemical*, 2013,

188, 1270-1276.

12. Q. He, Z. Zeng, Z. Yin, H. Li, S. Wu, X. Huang and H. Zhang, *Small*, 2012, **8**, 2994-2999.

13. Y. Zhang, A. Kolmakov, Y. Lilach and M. Moskovits, *The Journal of Physical Chemistry B*, 2005, **109**, 1923-1929.

14. J. Zhai, L. Wang, D. Wang, Y. Lin, D. He and T. Xie, *Sensors and Actuators B: Chemical*, 2012, **161**, 292-297.

15. P.-G. Su, C.-T. Lee, C.-Y. Chou, K.-H. Cheng and Y.-S. Chuang, *Sensors and Actuators B: Chemical*, 2009, **139**, 488-493.

16. X. Yu, C. Xie, L. Yang and S. Zhang, *Sensors and Actuators B: Chemical*, 2014, **195**, 439-445.

17. H.-D. Zhang, Y.-Z. Long, Z.-J. Li and B. Sun, *Vacuum*, 2014, **101**, 113-117.

18. J. Zhai, L. Wang, D. Wang, H. Li, Y. Zhang, D. Q. He and T. Xie, *ACS applied materials & interfaces*, 2011, **3**, 2253-2258.

19. R. Jiang, B. Li, C. Fang and J. Wang, *Adv Mater*, 2014, **26**, 5274-5309.

20. H. M. Chen, C. K. Chen, C.-J. Chen, L.-C. Cheng, P. C. Wu, B. H. Cheng, Y. Z. Ho, M. L. Tseng, Y.-Y. Hsu and T.-S. Chan, *ACS nano*, 2012, **6**, 7362-7372.

21. J. Brillet, M. Gratzel and K. Sivula, *Nano letters*, 2010, **10**, 4155-4160.

22. Z. Liu, W. Hou, P. Pavaskar, M. Aykol and S. B. Cronin, *Nano letters*, 2011, **11**, 1111-1116.

23. T. J. Meyer, *Nature*, 2008, **451**, 778-779.

24. Y. Li, H. Wang, Q. Feng, G. Zhou and Z.-S. Wang, *Energy & Environmental Science*, 2013, **6**, 2156.

25. M. D. Brown, T. Suteewong, R. S. S. Kumar, V. D'Innocenzo, A. Petrozza, M. M. Lee, U. Wiesner and H. J. Snaith, *Nano letters*, 2010, **11**, 438-445.

26. I. Thomann, B. A. Pinaud, Z. Chen, B. M. Clemens, T. F. Jaramillo and M. L. Brongersma, *Nano letters*, 2011, **11**, 3440-3446.

27. B. Wang, Z. Q. Zheng, L. F. Zhu, Y. H. Yang and H. Y. Wu, *Sensors and Actuators B: Chemical*, 2014, **195**, 549-561.

28. B. Wang, X. Jin and Z. B. Ouyang, *CrystEngComm*, 2012, **14**, 6888.

29. H. M. Dong, Y. H. Yang and G. W. Yang, *Materials Letters*, 2014, **115**, 176-179.

30. P. Rai, Y.-S. Kim, H.-M. Song, M.-K. Song and Y.-T. Yu, *Sensors and Actuators B: Chemical*, 2012, **165**, 133-142.

31. Y. Chen, D. Zeng, K. Zhang, A. Lu, L. Wang and D. L. Peng, *Nanoscale*, 2014, **6**, 874-881.

32. B. S. Passmore, D. C. Adams, T. Ribaudo, D. Wasserman, S. Lyon, P. Davids, W. W. Chow and E. A. Shaner, *Nano letters*, 2011, **11**, 338-342.

33. D. Zappa, E. Comini and G. Sberveglieri, *Nanotechnology*, 2013, **24**, 444008.

34. X. Wang, M. Zhao, F. Liu, J. Jia, X. Li and L. Cao, *Ceramics International*, 2013, **39**, 2883-2887.

35. H. Huang, H. Gong, C. L. Chow, J. Guo, T. J. White, M. S. Tse and O. K. Tan, *Advanced Functional Materials*, 2011, **21**, 2680-2686.

36. L. F. Zhu, J. C. She, J. Y. Luo, S. Z. Deng, J. Chen, X. W. Ji and N. S. Xu, *Sensors and Actuators B: Chemical*, 2011, **153**, 354-360.

37. D. Calestani, M. Villani, R. Mosca, L. Lazzarini, N. Coppede, S. C. Dhanabalan and A. Zappettini, *Nanotechnology*, 2014, **25**, 365502.

38. Q. Hao, L. Li, X. Yin, S. Liu, Q. Li and T. Wang, *Materials Science and Engineering: B*, 2011, **176**, 600-605.

39. I.-D. Kim, A. Rothschild, B. H. Lee, D. Y. Kim, S. M. Jo and H. L. Tuller, *Nano letters*, 2006, **6**, 2009-2013.

40. N. Barsan and U. Weimar, *Journal of Electroceramics*, 2001, **7**, 143-167.

41. J. Guo, J. Zhang, M. Zhu, D. Ju, H. Xu and B. Cao, *Sensors and Actuators B: Chemical*, 2014, **199**, 339-345.

42. S.-W. Fan, A. K. Srivastava and V. P. Dravid, *Applied Physics Letters*, 2009, **95**, 142106.

Figure Captions

Figure1. (a) The low magnifying FESEM image of the prepared ZnO NWs. The high-magnified FESEM images of (b) ZnO NWs and (c) Au-ZnO NWs. (d) Comparative XRD patterns of ZnO NWs and Au-ZnO NWs. UV–visible absorption spectra of the (e) ZnO NWs and (f) Au-ZnO NWs.

Figure 2. The 3D schematic diagrams of the (a) substrate, (b) sensor element. The photographs of the (c) side view and (d) top view of the sensor element package on a metal stent.

Figure 3. (a) Dynamics response of ZnO NWs sensor towards various concentrations of C_2H_2 at 130 ^oC in dark. Dynamics response of Au-ZnO NWs sensor towards various concentrations of C_2H_2 at room temperature for various conditions: (b) in dark; (d) under 532 nm light illumination; (f) under stronger visible light illumination. A close look of the resistance change of the Au-ZnO NWs sensor right after 200 ppm C_2H_2 gas pumped in (the inset is the full response curve to 200 ppm C_2H_2 gas) under different conditions: (c) in dark; (e) under 532 nm light illumination; (g) under stronger visible light illumination. (h) The response of Au-ZnO NWs sensor to 25-500 ppm C_2H_2 gas for various conditions at room temperature.

Figure 4. (a) Schematic energy-level diagrams of ZnO NWs, primitive (left), after heating (middle), and reaction with C_2H_2 gas (right). (b) Schematic energy-level diagrams of Au-ZnO NWs, primitive (left), reaction with little C_2H_2 gas (middle), and reaction with much C_2H_2 gas (right). (c) Schematic energy-level diagrams of Au-ZnO NWs under weak light irradiate (left), under stronger light irradiate (right) and reaction with C_2H_2 gas (middle).

Figure 1

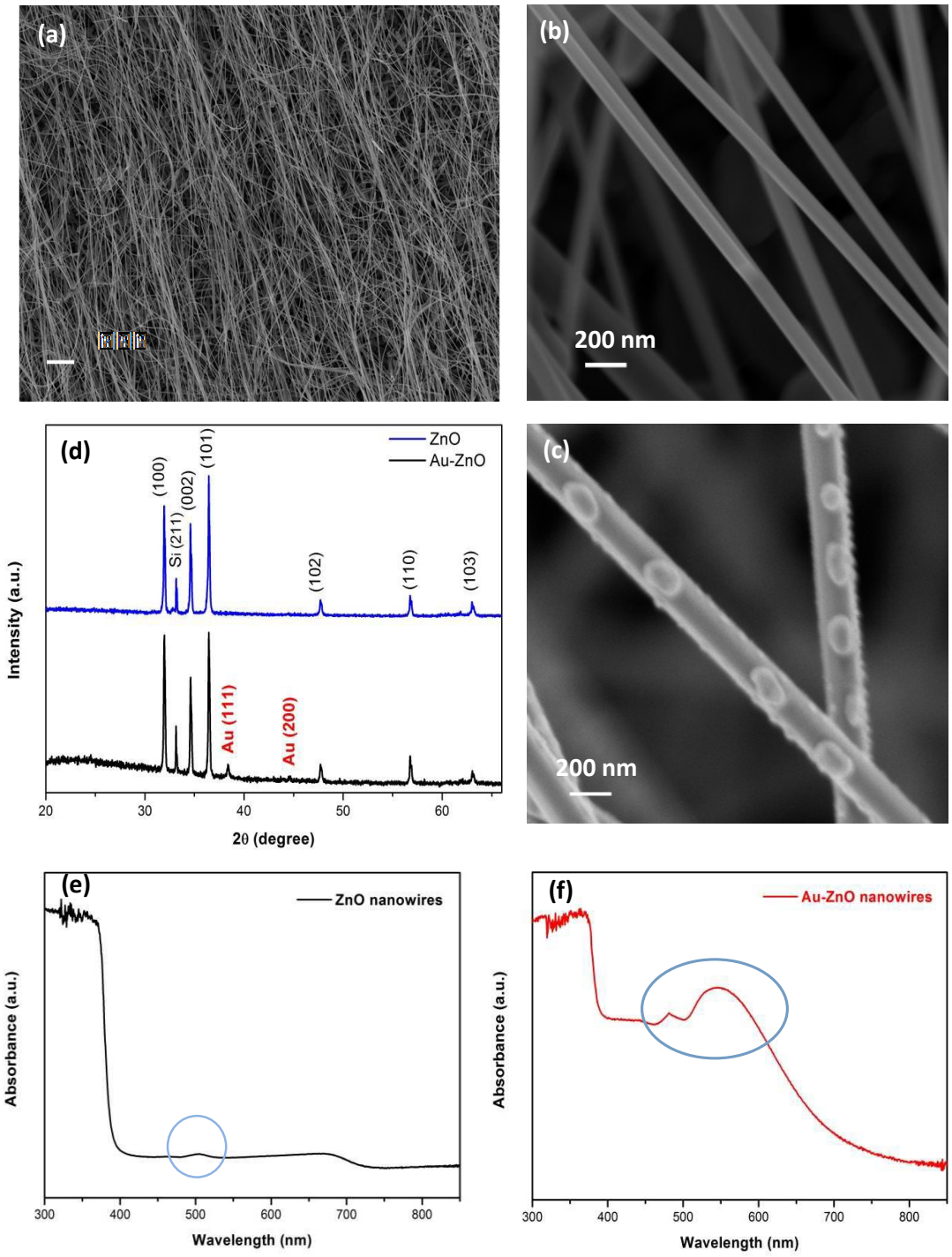

Figure 2

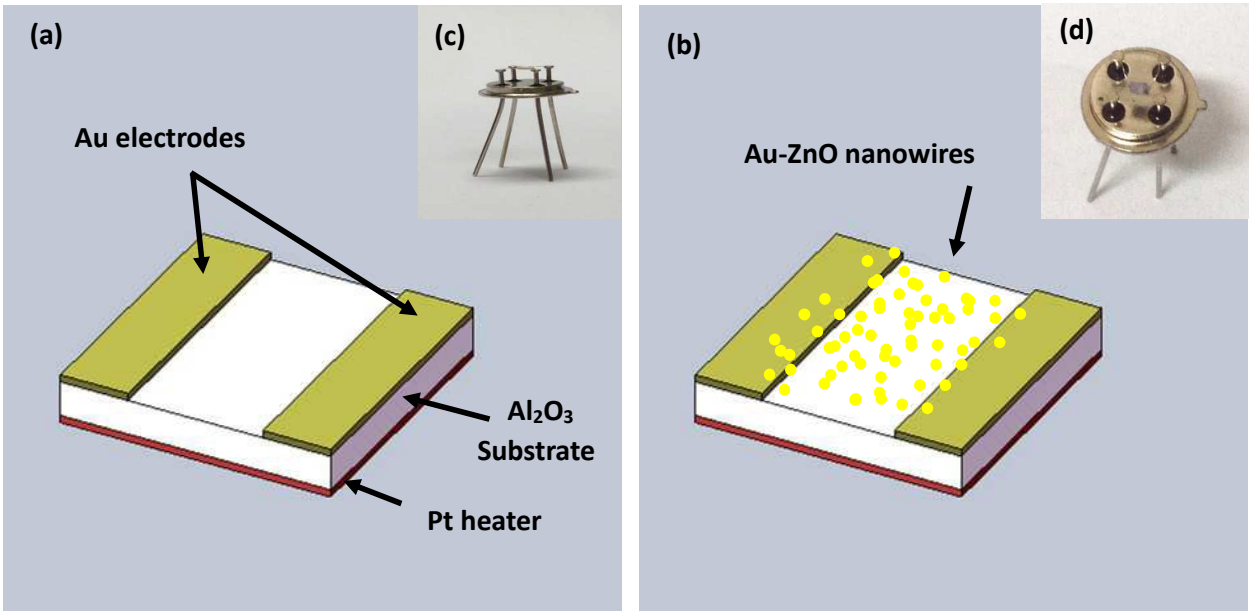

Figure 3

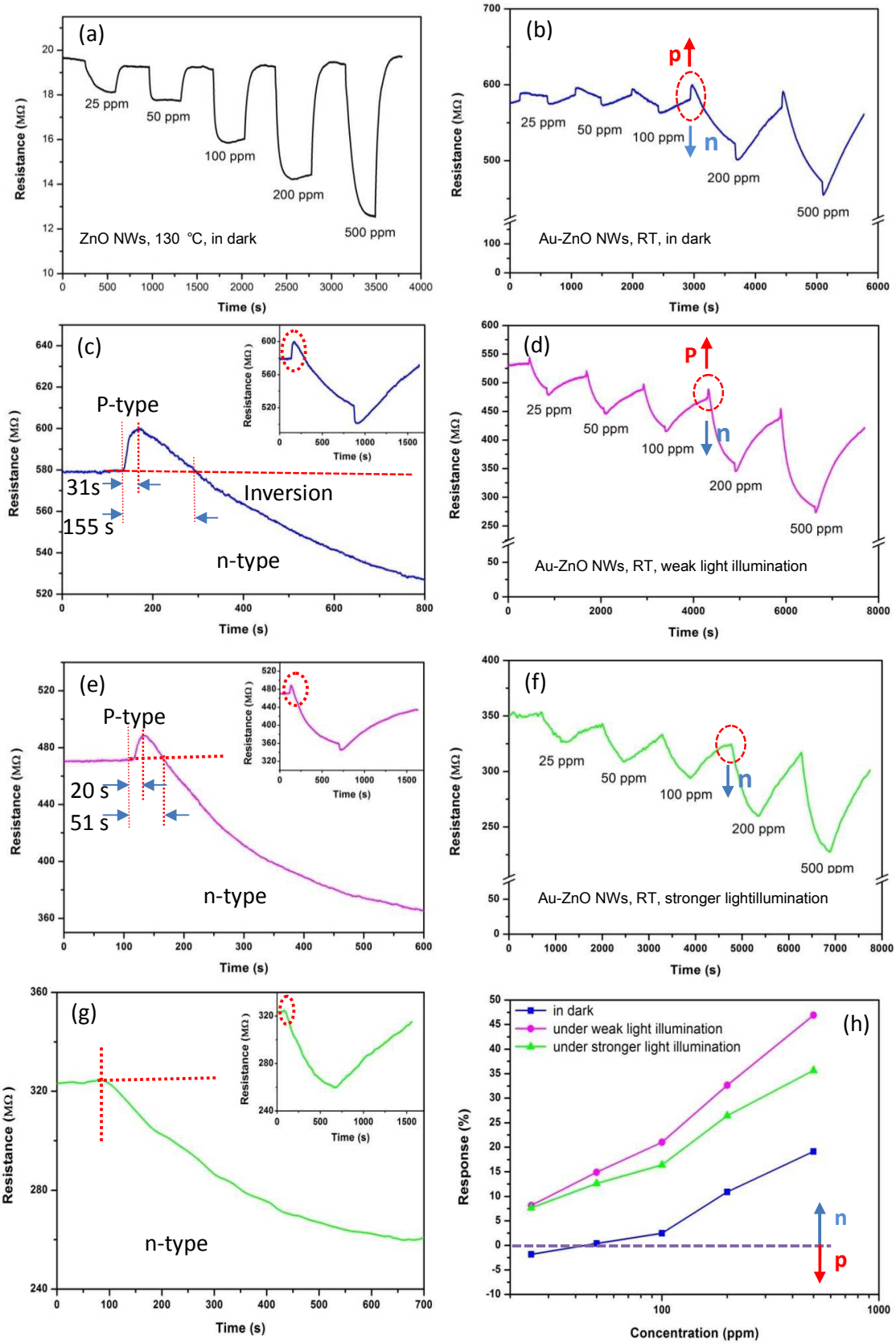

Figure 4

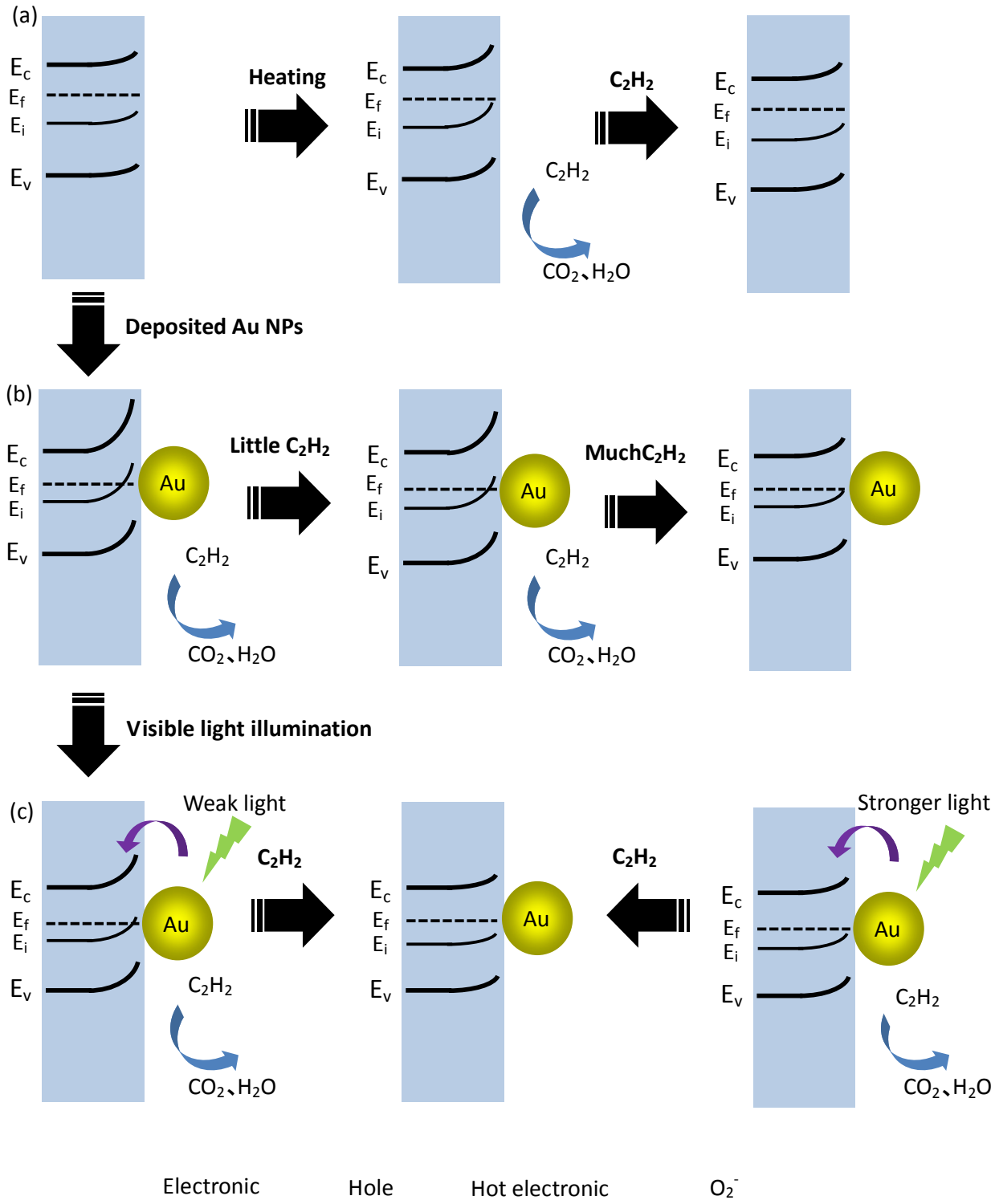

A table of contents entry

A visible light-controlled sensing response of the Au-ZnO nanowires for C_2H_2 gas at room temperature by the plasmon-enhanced sensitivity.